Published in final edited form as:
Chem Phys Lett. 2003 April 29; 372(3-4): 409–414. doi:10.1016/S0009-2614(03)00420-2.

Effects of metallic silver particles on the emission properties of $[Ru(bpy)_3]^{2+}$

Ignacy Gryczynski, **Joanna Malicka**, **Elisabeth Holder**, **Nicolas DiCesare**, and **Joseph R. Lakowicz***
Department of Biochemistry and Molecular Biology, Center for Fluorescence Spectroscopy, University of Maryland School of Medicine, 725 West Lombard Street, Baltimore, MD 21201, USA

Abstract

We examined the emission spectral properties of $[Ru(bpy)_3]^{2+}$ in a thin film of polyvinyl alcohol coated on quartz slides or on metallic silver particles. The relative intensities were several fold higher on the surface containing silver particles, and the decay times were several fold smaller. These results are consistent with an approximate 20-fold increase in the radiative decay rate of $[Ru(bpy)_3]^{2+}$ when near metallic silver particles. These results suggest the use of silver particles for increased detectability of the emission from transition metal–ligand complexes.

1. Introduction

We have recently reported the effects of metallic silver particles on nearby fluorophores [1, 2]. The conducting metallic surfaces change the photon mode density near the fluorophores and thus their emissive spectral properties of nearby fluorophores [3]. One remarkable consequences of the interaction is a potential increase in the radiative decay rate of a fluorophore. This rate is determined by the extinction coefficient of the fluorophore [4] and is typically insensitive to the local environment, similar to the absorption spectra. Our experiment studies [2] have demonstrated apparent increases in quantum yield and decreased lifetime near silver particles, which is consistent with increases in the radiative decay rates.

We are not aware of studies of the effects of silver particles on metal–ligand complexes. In the present report we extended these studies to the transition metal–ligand complex $[Ru(bpy)_3]^{2+}$, where bpy is 2,2′-bipyridyl. Complexes of Ru, Re and Os with diimine ligands have been extensively studied for use in solar energy conversion. Additionally, these compounds are used for electrochemiluminescent assays in macromolecular systems [5,6] and more recently as luminescence probes in biochemistry, biophysics and biotechnology [7–11]. These applications of metal–ligand complexes (MLCs) are valuable because of the long luminescent decay times of the MLCs, which vary from 10 ns to 10 μs [12,13]. Because of these important applications of MLCs to biochemistry and biotechnology, and the growing interest in the applications of metal-enhanced fluorescence [14,15], we examined the intensities and lifetimes of $[Ru(bpy)_3]^{2+}$ near silver particles.

2. Materials and methods

2.1. Surface preparation and silver island films

Quartz slides were used as substrates. The use of quartz provided UV transmission and less autofluorescence than glass. The quartz slides were soaked in a 10:1 (v/v) mixture of H_2SO_4

*Corresponding author. Fax: 1-410-7068408. E-mail address: lakowicz@umbi.umd.edu (J.R. Lakowicz).

(95–98%) and H_2O_2 (30%) overnight before silver deposition, washed with distilled water, and air-dried prior to use. Silver island films (SIFs) were deposited by reduction of silver nitrate with D-glucose, as described previously [2,16]. Half of the slide area was covered with the SIF. The unsilvered half was used as the control. The entire slide was coated with $[Ru(bpy)_3]^{2+}$ in a polyvinyl alcohol (PVA) film. The PVA film was prepared by spin coating at 5000 rpm for 2 min a 1 mM solution of $[Ru(bpy)_3]^{2+}$ in 0.2% PVA (Aldrich, MW 16 000–23 000) in water.

2.2. Fluorescence measurements

Our sample configuration is shown in Fig. 1 (top panel). The slide was placed in a quartz cuvette with a sealed top which allowed flushing with the desired gas, as described in [17]. Emission spectra were obtained using a Varian Eclipse spectrofluorometer using 465 nm excitation. Intensity decays were measured in the frequency- domain using instrumentation described previously [18] using an amplitude-modulated blue LED as the excitation source. The LED output was filtered to obtain 450–480 nm. The emission was observed through a combination long pass 550 nm filter and a 610 ± 20 nm interference filter.

For frequency-domain measurements the excitation was vertically polarized and the emission observed through a polarizer oriented at 54.7° from the vertical position. The FD intensity decay were analyzed in terms of the multi-exponential model

$$I(t)=\sum_i \alpha_i \exp(-t/\tau_i), \tag{1}$$

where τ_i are the lifetimes with amplitudes α_i and $\Sigma\ \alpha_i = 1.0$. Fitting to the multi-exponential model was performed as described previously [19]. The contribution of each component to the steady state intensity is given by

$$f_i=\frac{\alpha_i\tau_i}{\sum_j \alpha_j\tau_j}. \tag{2}$$

The mean decay time is given by

$$\bar{\tau}=\sum_i f_i\tau_i. \tag{3}$$

The amplitude-weighted lifetime is given by

$$\langle\tau\rangle=\sum_i \alpha_i\tau_i. \tag{4}$$

If the sum of the α_i values are not normalized, and all instrument parameters are unchanged, then the value of $\langle\tau\rangle$ is proportional to the total steady state intensity.

3. Results

Sub-wavelength size metallic silver particles display a strong absorption with a maximum near 480 nm (Fig. 1). This absorption is due to the electron oscillations induced by the incident light field, and is called the surface plasmon resonance [20]. The AFM image of a typical SIF used for this study (Fig. 2) shows silver particles ranging in size from 20 to 80 nm high.

We examined the emission spectra of $[Ru(bpy)_3]^{2+}$ in PVA on quartz (Q) and on SIFs (S). Quenching by oxygen occurs on both the quartz and SIF surfaces (Table 1). In an argon atmosphere the emission intensity of $[Ru(bpy)_3]^{2+}$ is about 7-fold larger on the SIF than on quartz (Fig. 3). Comparable increases in intensity were observed in an atmosphere of air or oxygen.

Changes in the rate of radiative decay can be detected by decrease in the lifetime [1,2]. Hence, we measured the frequency-domain (FD) intensity decay of $[Ru(bpy)_3]^{2+}$ in each atmosphere, and on quartz and on SIFs (Fig. 4). In each case there is a decreased lifetime on the SIFs. A decreased lifetime with an increased intensity (Fig. 3) indicates an increase in the rate of radiative decay of $[Ru(bpy)_3]^{2+}$. Based on the intensity decays in Fig. 4, and ellipsometry for similar spin-coated samples [21], we estimate the average film thickness to be in the range of 10 nm, but this estimate has considerable uncertainties.

The FD intensity decays were analyzed in terms of the multi-exponential model (Eq. (1)) and the results summarized in Table 2. Examination of these data reveal that the individual decay times, averages lifetime and amplitude-weighted lifetimes are shorter on SIFs than on quartz. Decreases in lifetime are observed in argon, air or oxygen. Increased intensities (Fig. 3) and decreased lifetimes is strong evidence for an increase in the radiative decay rate.

It is of interest to use the intensity (Fig. 3) and lifetime data (Table 2) to estimate the increase in the radiative decay rate of $[Ru(bpy)_3]^{2+}$ on silver island films. This can be accomplished by using the definitions of the quantum yield (Q_0) and lifetime (τ_0) on the quartz surface

$$Q_0=\frac{\Gamma}{\Gamma+k}, \tag{5}$$

$$\tau_0=\frac{1}{\Gamma+k}, \tag{6}$$

where γ is the radiative decay rate and k is the sum of the non-radiative decay rates. Using these expressions the radiative decay rate on quartz is given by

$$\Gamma=Q_0/\tau_0. \tag{7}$$

Now assume that proximity of $[Ru(bpy)_3]^{2+}$ to the SIFs results in an increase in the affected radiative decay rate to Γ_m. Assuming the non-radiative rates k are not changed due to the SIFs, the quantum yields and lifetimes near the metal (m) are given by

$$Q_m = \frac{\Gamma_m}{\Gamma_m + k}, \tag{8}$$

$$\tau_m = \frac{1}{\Gamma_m + k}, \tag{9}$$

so that

$$\Gamma_m = \frac{Q_m}{\tau_m}. \tag{10}$$

It is difficult to estimate the absolute quantum yields for $[Ru(bpy)_3]^{2+}$ in the thin PVA films. However, if ratios are used, the quantum yields can be replaced with the relative intensities (I_0 and I_m), assuming the SIFs have a minimal effect on the rate of excitation. Hence the ratios of Γ_m/Γ can be calculated using

$$\frac{\Gamma_m}{\Gamma} = \frac{\tau_0}{\tau_m}\frac{I_m}{I_0}. \tag{11}$$

The calculated values of Γ_m/Γ are summarized in Table 2. This ratio was calculated using both the mean lifetime $\bar{\tau}$ and the amplitude-weighted lifetimes $\langle\tau\rangle$. While it is not presently clear which type of weighted average lifetime should be used, the results are the same. The radiative decay rate of $[Ru(bpy)_3]^{2+}$ increases about 20-fold when coated on silver island films. We stress that there are apparent values spatially averaged over these illuminated region of the sample and the thickness of the PVA film. Also, our calculation assumes no change in the rates of excitation or non-radiative decay. Even if the rate of excitation changed, this does not alter our conclusion that the emission intensities are higher and lifetime of $[Ru(bpy)_3]^{2+}$ are smaller on SIFs than on quartz.

4. Discussion

It is of interest to consider the implications of the changes in quantum yield and lifetime for fluorophore detectability. Suppose the sample is observed in the linear excitation region where there is no significant ground state depletion. Assuming there is no change in the rate of excitation, the number of photons/second is increased by a factor Q_m/Q_0 or equivalently I_m/I_0 if the rate of excitation is not changed by the SIF. If the fluorophore is observed continuously until photobleached then the number of observed photons should increase by a factor of τ_0/τ_m due to less time for photobleaching during each excitation–deexcitation cycle. Hence the number of observable photons for $[Ru(bpy)_3]^{2+}$ is expected to increase by the product of these factors, or about 20-fold.

Now consider the case of saturating light conditions. In this case the number of photons per second will be increased by factors of Q_m/Q_0 and τ_0/τ_m, where the latter factor τ_0/τ_m is the result of more rapid cycling of the molecules. Additionally, the decreased lifetime will also result in decreased photobleaching. Hence, the total increase in observed photons, when accumulated till photobleached, will be increased by $(Q_m/Q_0)(\tau_0/\tau_m)$ (τ_0/τ_m) which for $[Ru(bpy)_3]^{2+}$ is about

a factor of 80-fold. These considerations suggest that the use of metallic particles can result in substantial improved detectability of fluorophores.

Acknowledgments

This work was supported by the National Institute of Biomedical Imaging and Bioengineering NIH EB-00682 and the National Center for Research Resources, RR-08119.

References

1. Lakowicz JR. Anal Biochem 2001;298:1. [PubMed: 11673890]
2. Lakowicz JR, Shen Y, D'Auria S, Malicka J, Fang J, Gryczynski Z, Gryczynski I. Anal Biochem 2002;301:261. [PubMed: 11814297]
3. Barnes WL. J Mod Opt 1998;45(4):661.
4. Strickler SJ, Berg RA. J Chem Phys 1962;37:814.
5. Miller CJ, McCord P, Bard AJ. Langmuir 1991;7:2781.
6. Blackburn GF, Shah HP, Kenten JH, Leland J, Kamin RA, Link J, Peterman J, Powell MJ, Shah A, Talley DB, Tyaki SK, Wilkins E, Wy TG, Massey RJ. Clin Chem 1991;37:1534. [PubMed: 1716534]
7. Terpetschnig E, Szmacinski H, Malak H, Lakowicz JR. Biophys J 1995;68:342. [PubMed: 7711260]
8. Szmacinski H, Terpetschnig E, Lakowicz JR. Biophys Chem 1996;62:109. [PubMed: 8962474]
9. Gryczynski I, Gryczynski Z, Rao G, Lakowicz JR. Analyst 1999;124:1041. [PubMed: 10736861]
10. Kusba J, Li L, Gryczynski I, Piszczek G, Johnson ML, Lakowicz JR. Biophys J 2002;82:1358. [PubMed: 11867452]
11. Lakowicz, JR.; Gryczynski, I.; Piszczek, G.; Tolosa, L.; Nair, R.; Johnson, ML.; Nowaczyk, K. Methods in Enzymology. Vol. 323. Academic Press; New York: p. 473
12. Juris A, Galzani V, Barigelletti F, Campagna S, Belser P, Von Zelewsky A. Coord Chem Rev 1988;84:85.
13. Demas, JN.; DeGra, BA. Topics in Fluorescence Spectroscopy, Probe Design and Chemical Sensing. Lakowicz, JR., editor. Vol. 4. Plenum Press; New York: 1994. p. 71
14. Schalkhammer T, Aussenegg FR, Leitner A, Brunner H, Hawa G, Lobmaier C, Pittner F. SPIE 1997;2976:1290.
15. Lobmaier, Ch; Hawa, G.; Gotzinger, M.; Wirth, M.; Pittner, F.; Gabor, F. J Mol Recognit 2001;14:215. [PubMed: 11500967]
16. Sokolov K, Chumanov G, Cotton TM. Anal Chem 1998;70:3898. [PubMed: 9751028]
17. Gryczynski I, Gryczynski Z, Rao G, Lakowicz JR. Analyst 1999;124:1041. [PubMed: 10736861]
18. Laczko G, Gryczynski I, Gryczynski Z, Wiczk W, Malak H, Lakowicz JR. Rev Sci Instrum 1990;61:2331.
19. Lakowicz JR, Laczko G, Cherek H, Gratton E, Limkeman M. Biophys J 1994;46:463. [PubMed: 6498264]
20. Kerker M. J Colloid Interface Sci 1985;105:297.
21. Holder E, DiCesare N, Gryczynski Z, Briggman K, Malicka J, Gryczynski I, Lakowicz JR. in preparation.

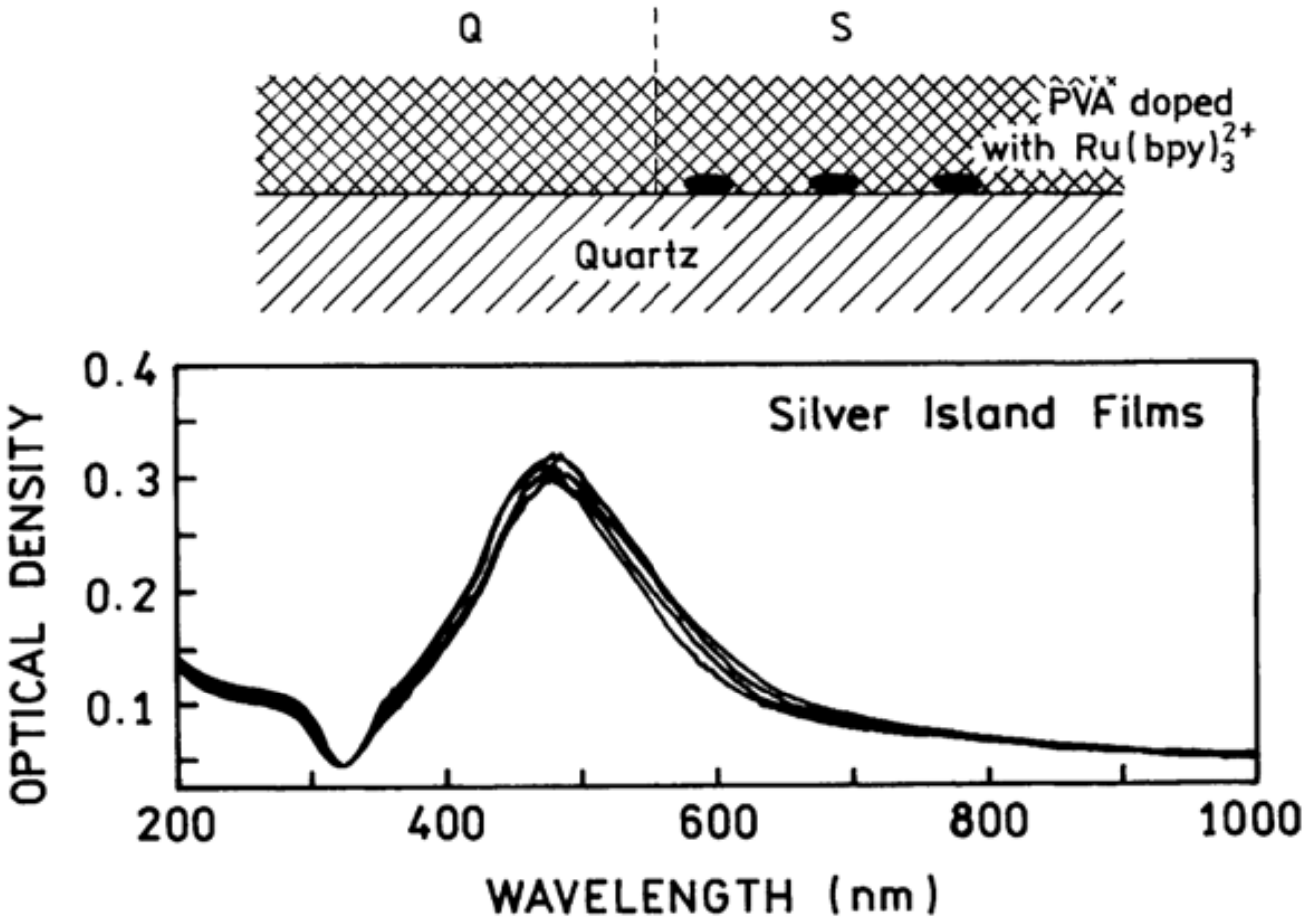

Fig. 1.
Absorption spectra of four SIFs from a single preparation, showing the consistency of the SIFs. The upper panel shows our sample geometry.

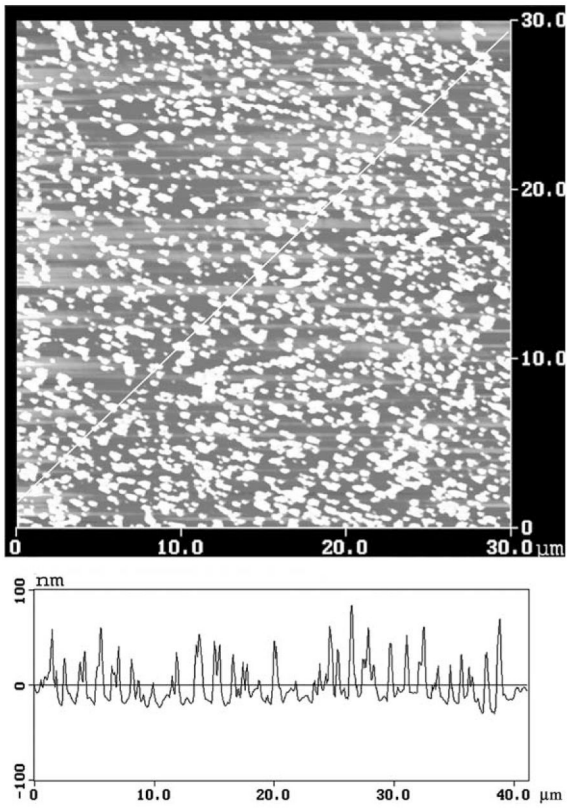

Fig. 2.
Atomic force microscope image of a quartz slide coated with a silver island film.

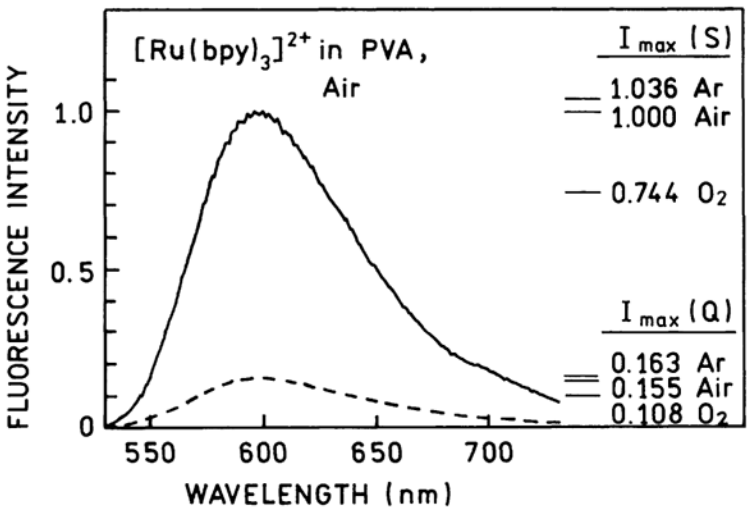

Fig. 3.

Emission spectra and relative intensities of $[Ru(bpy)_3]^{2+}$ in PVA on quartz (Q) and silver island films (S). The horizontal lines show the emission intensities in argon, air or an oxygen atmosphere.

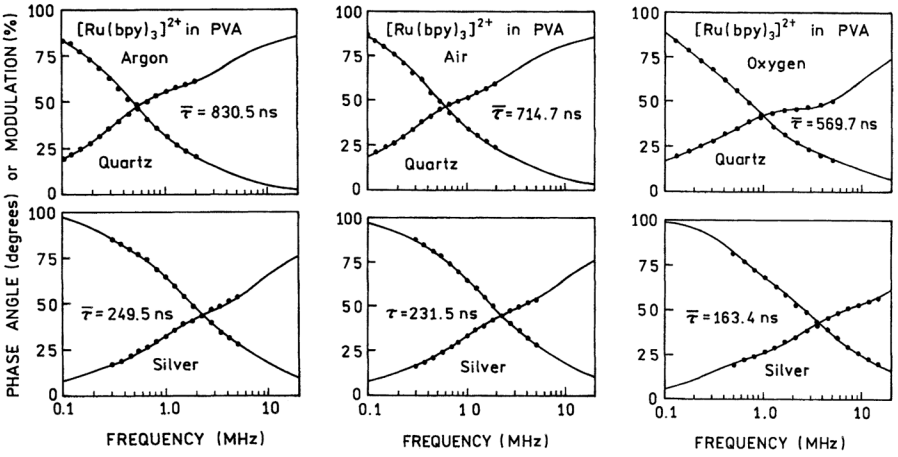

Fig. 4.

Frequency-domain intensity decays of $[Ru(bpy)_3]^{2+}$ in PVA equilibrated with an argon, air or oxygen atmosphere. Top panels, on quartz. Bottom panels, on silver islands.

Table 1

Calculation of the apparent increase in the radiative decay rate of $[Ru(bpy)_3]^{2+}$

Conditions	$\langle\tau_0\rangle/\langle\tau_m\rangle$	I_0/I_m	Γ_m/Γ
Argon	3.84	6.36	24.2
Air	3.46	6.45	22.3
O_2	2.61	6.88	18.0
	$\bar{\tau}_0/\bar{\tau}_m$	I_0/I_m	Γ_m/Γ
Argon	3.33	6.36	21.5
Air	3.09	6.45	19.9
O_2	3.48	6.88	23.9

Table 2

Multi-exponential analysis of $[Ru(bpy)_3]^{2+}$ intensity decays in absence and presence of silver island films

Conditions	$\bar{\tau}$ (ns)	$\langle\tau\rangle$ (ns)	α_1	f_1	τ_1 (ns)	α_2	f_2	τ_2 (ns)	α_3	f_3	τ_3 (ns)	χ_R^2
Air, quartz	714.7[a]	250.4[b]	0.629	0.178	70.3	0.338	0.579	428.0	0.033	0.243	1863	1.4 (724.7)[c]
Air, silver	231.5	72.3	0.680	0.219	23.4	0.300	0.578	140.2	0.020	0.203	716.8	1.8 (694.81)
Argon, quartz	830.5	280.0	0.553	0.117	59.1	0.409	0.605	412.6	0.038	0.278	2065	1.5 (661.8)
Argon, silver	249.5	73.0	0.693	0.230	24.2	0.283	0.540	137.5	0.024	0.236	722.4	1.8 (772.2)
O_2, quartz	569.7	101.6	0.771	0.162	21.3	0.193	0.432	226.7	0.036	0.406	1151	2.5 (2516)
O_2, silver	163.4	39.0	0.644	0.139	8.1	0.309	0.444	53.8	0.047	0.417	331.9	3.4 (1294)

[a] $\bar{\tau}=\sum_i f_i\tau_i$.

[b] $\langle\tau\rangle=\sum_i \alpha_i\tau_i$.

[c] Numbers in parenthesis are χ_R^2 values for one-exponential fit.